J Infect Chemother 25 (2019) 96–103

Contents lists available at ScienceDirect

Journal of Infection and Chemotherapy

journal homepage: http://www.elsevier.com/locate/jic

Original Article

Identification and antifungal sensitivity of two new species of *Diaporthe* isolated☆,☆☆

Kenji Ozawa [a,*], Kiyofumi Mochizuki [a], Daisuke Takagi [a], Kyoko Ishida [b], Atsuko Sunada [c], Kiyofumi Ohkusu [d], Katsuhiko Kamei [e], Akira Hashimoto [f,1], Kazuaki Tanaka [f]

[a] Department of Ophthalmology, Gifu University Graduate School of Medicine, Gifu, Japan
[b] Department of Ophthalmology, Toho University Ohashi Medical Center, Tokyo, Japan
[c] Department of Medical Technology, Osaka University Hospital, Osaka, Japan
[d] Department of Microbiology, Tokyo Medical University Graduate School of Medicine, Tokyo, Japan
[e] Division of Clinical Research, Medical Mycology Research Center, Chiba University, Chiba, Japan
[f] Faculty of Agriculture and Life Science, Hirosaki University, Aomori, Japan

ARTICLE INFO

Article history:
Received 27 July 2018
Received in revised form
19 September 2018
Accepted 11 October 2018
Available online 10 November 2018

Keywords:
Keratomycosis
Diaporthe
Phylogeny
Taxonomy

ABSTRACT

Diaporhte species are plant pathogens rarely involved in human diseases, especially eye diseases. We report our findings in two undescribed *Diaporhte* species. Both were identified by their morphological characteristics and by DNA sequence analyses. In Case 1, an 81-year-old male farmer who had pterygium surgery 7 years earlier developed keratitis and the causal fungus was identified as a new species of *Diaporthe*, *D. oculi*. This species can be distinguished from the closely related *D. limonicola* on *Citrus limon* (Rutaceae) by the ITS, *tef1*, and *TUB* (515/520 = 99.0% in ITS, 315/324 = 97.2% in *tef1*, and 601/614 = 97.9% in *TUB*). The isolate from Case 2, a 68-year-old man with a rose thorn injury, was also identified as a new *Diaporthe* species, *D. pseudooculi*. Phylogenetically, *D. pseudooculi* is different from the closely related *D. podocarpi-macrophylli* by the ITS, *tef1*, and *TUB* (525/531 = 98.9% in ITS, 314/333 = 94.3% in *tef1*, and 436/442 = 98.6% in *TUB*).

We report on the identification, drug sensitivity, and treatment outcomes for these two new species of *Diaporthe*, *D. oculi* and *D. pseudooculi*.

1. Introduction

Mycotic keratitis is a rare and serious corneal infection generally found in the tropical and subtropical regions [1,2]. Although *Fusarium*, *Aspergillus,* and *Candida* are common human pathogens, the *Diaporthe* species which are widely present in plants and soil are rarely cause human disease. Eight cases with *Diaporthe* species infections have been reported previously [3–10]; 2 cases with osteomyelitis [3,4], 3 with cutaneous infections [5–7], and 1 with bursitis [8]. For ocular infections, only two cases have been reported [9,10]. We presented two new Diaporthe species that have not been described as ocular pathogens.

2. Materials and methods

2.1. Case presentation

2.1.1. Case 1

An 80-year-old male farmer visited an eye clinic for an uncomfortable sensation oculus sinister (OS). He was diagnosed with keratitis and treated with topical antibiotics (1.5% levofloxacin, 0.3% tobramycin and 0.5% cefmenoxime) and steroids (0.1% betamethasone). Because the keratitis did not improve, he was referred to our hospital, ten days later.

The examination indicated that there was no history of ocular trauma caused by soil or plants, but he had cataract surgery with

☆ All authors meet the ICMJE authorship criteria.

☆☆ TreeBASE Reviewer access URL: http://purl.org/phylo/treebase/phylows/study/TB2:S22393?x-access-code=86a9457c5badbc76740c611b0325c1a9&format=html.

* Corresponding author. Gifu University Graduate School of Medicine, 1-1 Yanagido, Gifu-shi 501-1194, Japan.
E-mail address: kj-ozawa@umin.ac.jp (K. Ozawa).
[1] Present address: Japan Collection of Microorganisms, RIKEN BioResource Research Center, Ibaraki, Japan.

https://doi.org/10.1016/j.jiac.2018.10.008
1341-321X/

removal of a pterygium more than 7 years earlier. His best-corrected visual acuity (BCVA) was 20/20 oculus dexter (OD) and 20/250 OS. Slit-lamp examination showed a grayish-white, ring-shaped infiltrate in the central cornea with mild conjunctival injection (Fig. 1A). The left fundus was not visible because of the corneal opacity. Microscopic examination of corneal scrapings revealed no signs of bacteria or fungi. Laboratory tests showed no signs of systemic inflammation. We tentatively diagnosed the patient with bacterial keratitis and began treatment with intravenous meropenem, topical levofloxacin and cefmenoxime, and subconjunctival injections of vancomycin and ceftazidime. Because Sabouraud agar plates inoculated with corneal scrapings showed fungal filaments seven days later, he was diagnosed with keratomycosis. The treatment was replaced to topical 1% voriconazole (VRCZ), 0.1% amphotericin B (AMPH-B), and 5% pimaricin every hour, and intravenous VRCZ (400 mg/day). He was also given daily subconjunctival injections of 1% VRCZ followed by corneal stromal injections of 1% VRCZ. Since his liver enzymes were elevated on the 14th day, VRCZ was replaced to intravenous liposomal amphotericin B (L-AMB). The size of the corneal lesion decreased, but the patient developed L-AMB-related hypokaremia on the 22nd day. Therefore, we performed therapeutic penetrating keratoplasty with a trephine 1 mm larger than the area of fungal infection to remove the infected cornea. After the surgery, a lower-than-standard dose of intravenous VRCZ (100 mg/day) was started and the topical VRCZ was continued.

One week after the surgery, fungal keratitis was confirmed from the excised corneal specimen, and there were no fungal elements at the edge of the tissue (Fig. 1B). The aqueous humor culture was negative. Then, we supplemented the treatment with topical corticosteroid (0.1% fluorometholone) and oral dexamethasone (2 mg/day) which were tapered over 1 week. Systemic antifungal therapy (VRCZ: 100 mg/day) was gradually reduced. His BCVA had improved to 10/20 OS. No further reactivation of the fungal infection was observed while continuing with the topical antifungal and corticosteroid (0.1% fluorometholone) for 18 months.

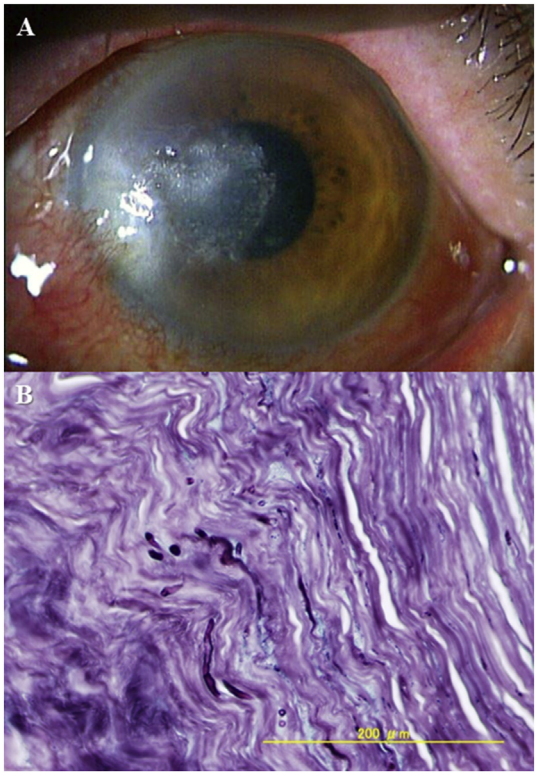

Fig. 1. Case 1. Findings in a patient with keratomycosis. A: Slit-lamp photograph at presentation showing infected cornea. B: Photomicrograph of a histologic section of infected cornea obtained after therapeutic penetrating keratoplasty. Grocotto-Gomori silver staining demonstrating positive elements in the corneal stroma. There are no fungal elements at the margins of the removed corneal tissue.

2.1.2. Case 2

A 68-year-old man visited our hospital complaining of severe eye pain and hyperemia OS. He had a rose thorn injury OS while gardening on the previous day. Our examination showed that BCVA was hand motion OS and 20/20 OD. Slit-lamp examination demonstrated severe conjunctival hyperemia, corneal infiltrate related to a retained foreign body, probably the thorn, and severe fibrin deposits and hypopyon in the anterior chamber (Fig. 2). We could not determine how deep the foreign body embedded itself in the cornea because of corneal clouding and severe anterior chamber reaction. There were no signs of opacities in the vitreous by B-mode ultrasonography. Laboratory tests showed no signs of systemic inflammation. A complete removal of the foreign body was impossible, and the excised specimens were submitted for microbiological culture. Topical levofloxacin and cefmenoxime and intravenous cefozopran were administered.

Five days later, *Pantoea sp.* was identified, and it was susceptible to almost all antibiotics except ampicillin. We continued the initial antibacterial therapy, and corneal clouding and anterior chamber reaction gradually reduced. Because a remnant of the thorn which had perforated into the anterior chamber was seen, additional surgery to remove the thorn fragment was performed on the 10th day. A soft contact lens was used for wound leakage after the surgery.

Because a filamentous fungus was identified from the removed specimen, the treatment was switched to topical 1% VRCZ and 0.1% AMPH-B, 5% pimaricin ointment, and intravenous VRCZ (400 mg/day). The corneal wound gradually healed and he was discharged 2 weeks after the beginning of the antifungal therapy. At the 2-month follow-up, the corneal lesion had healed leaving a mild scar. His BCVA was 4/200 OS because of the development of a cataract. No further reactivation of the fungal infection has been observed during the following 8-month with the antifungal therapy (topical 1% VRCZ).

2.2. Fungal strain

The two strains were cultured on Sabouraud dextrose agar plates and incubated at 25 °C for 7 days in Gifu University. Samples were sent to Hirosaki University for species identification. Cultures were deposited in the Japan Collection of Microorganisms (JCM),

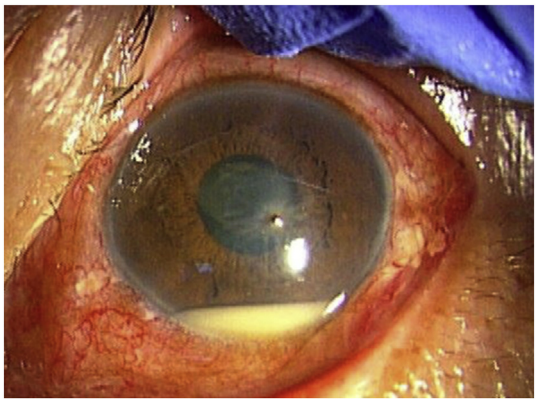

Fig. 2. Case 2. Findings in a patient with keratomycosis. Slit-lamp photograph at the time of presentation showing corneal foreign body, and hypopyon.

and the Genebank Project of NARO, Japan (MAFF). Specimens were deposited in the Herbarium of Hirosaki University, Fungi (HHUF).

2.3. Morphological analyses

Macro- and micromorphology and growth characteristics of the isolates were studied by the methods described by Tanaka et al. [11]. Briefly, the induction of sexual or asexual fructification was attempted by culturing the isolates on rice straw agar and/or incubating small pieces of the colony in sterilized water. Morphological characters were observed by differential interference and phase contrast microscopy (Olympus BX53), with images recorded with an Olympus digital camera (DP21).

2.4. DNA extraction and amplification

Mycelia were grown in potato dextrose agar (20 g potato extract, 20 g dextrose, 1000 mL distilled water), and the DNA of the mycelia was extracted using the ISOPLANT Kit II (Nippon Gene, Japan) according to the manufacturer's instructions. The complete internally transcribed spacers (ITS) regions of the nrDNA, the intron sequence of the transcription elongation factor (*tef1*) gene, and the partial beta tubulin (*TUB*) region were sequenced to determine their phylogenetic position at the generic and species level. These regions were amplified by polymerase chain reaction (PCR) using the primer pairs:

ITS = ITS1/ITS4 [12], *tef1* = EF1-728F/EF1-986R [13], and *TUB* = T1/Bt2b [14,15].

Amplifications were performed in 25 μL volumes consisting of 2 μL DNA, 2.5 μL of 10 × TEMPase Buffer I, 2.5 μL of 10 mM dNTP mix, 1 μL of each primer (20 pM), 1 μL of 25 mM $MgCl_2$, 14.5 μL MilliQ water, and 0.5 μL TEMPase Hot Start DNA polymerase (Ampliqon, Denmark). PCR was carried out on a PC 320 thermocycler (ASTEC, Japan) as follows: 95 °C for 15 min, 35 cycles of 1 min at 94 °C, 1 min at the designated annealing temperature (61.5 °C for ITS, 47 °C for *tef1*, and 58 °C for *TUB*), and 1 min at 72 °C, with a final denaturation step of 7 min at 72 °C. The PCR products were sequenced directly at SolGent Co., Ltd. (South Korea).

2.5. Phylogenetic analyses

The sequences derived from this study were deposited in the GenBank. First ITS sequences BLAST search on GenBank (http://www.ncbi.nlm.nih.gov/genbank/) suggested the two strains were phylogenetically related to *D. arecae* complex (data not shown). All sequences were aligned using the MAFFT version 7 [16]. Phylogenetic analyses were conducted using maximum likelihood (ML) and Bayesian methods. The optimum substitution models for each dataset were estimated using the Kakusan4 program [17] based on the Akaike information Criterion (AIC; [18]) for the ML analysis, and the Bayesian Information Criterion (BIC; [19]) for the Bayesian analysis. The ML analysis was performed using the RAxML-HPC2 v. 8.2.10 on Cipres Sience Gateway [20,21] based on the models selected with the AICc4 parameter (a proportional model among genes and codons). GTR + G was used for ITS, *tef1*, and *TUB*. Bootstrap proportions (BPs) were obtained via 1000 bootstrap replicates. Bayesian analysis was performed with MrBayes v. 3.2.6 on Cipres Sience Gateway [20,22] using substitution models containing the BIC4 parameter (i.e., proportional codon proportional model).

SYM was used for ITS, HKY85 for *tef1*, and HKY85 for *TUB*. Two simultaneous and independent Metropolis-coupled Markov-chain Monte Carlo (MCMC) runs were performed for 2 M generations with the tree sampled every 1000 generations for the analyses. Convergence of the MCMC procedure was assessed from the average standard deviation of the split frequencies (<0.01) and effective sample size scores (all >100) using MrBayes and Tracer v. 1.6 [23], respectively. The first 25% of the trees were discarded as burn-in, and the remainder were used to calculate the 50% majority-rule trees and to determine the posterior probabilities (PPs) for individual branches. *Diaporthe decedens* was used as outgroup according to phylogenies of [24]. These alignments were submitted to TreeBASE under study number S22393.

2.6. In vitro antifungal susceptibility testing

The minimal inhibitory concentrations (MICs) of the isolates were confirmed by the broth microdilution method at Osaka University Hospital. We used an order-made kit, Frozen Plate for Antifungal Susceptibility Testing of corneal infection (Eiken Chemical Co., Ltd., Tokyo). The drugs used were AMPH-B (0.03–16 μg/mL), flucytosine (0.12–64 μg/mL), fluconazole (FLCZ; 0.12–64 μg/mL), itraconazole (ITCZ; 0.015–8 μg/mL), miconazole (0.03–16 μg/mL), micafungin (MCFG; 0.015–16 μg/mL), VRCZ (0.015–8 μg/mL), and pimaricin (0.03–16 μg/mL). Because there was no established method of testing the susceptibility of the *Diaporthe* species, we performed that by the following conditions. Because the conidia-forming ability was low on potato dextrose agar, and adequate amounts of conidia could not be collected, we collected conidia and hyphae together by scraping the colony with an inoculating loop and used the mixture for MIC determination. Then the number of mycelia along with conidia in the inoculum was counted using a hemocytometer (BurkereTurk cell counter) and adjusted to a final concentration of 0.4×10^4 cfu/mL. Because this fungus did not grow at 35 °C, the plates were incubated at 25 °C, and the MICs were read after 48 h when growth of the control was well observed. These culture conditions referred to the CLSI M38-A2 standard.

3. Results

3.1. Phylogenetic analyses

ML and Bayesian phylogenetic analyses were conducted using an aligned sequence dataset comprised of 642 nucleotide positions from *TUB*, 503 from ITS, and 364 from *tef1*. The alignment contained a total of 37 taxa which consisted of 37 taxa in *TUB*, ITS, and *tef1*. The combined dataset provided higher confidence values for the generic and species levels than did those of the individual gene trees. Of the 1558 characters included in the alignment, 515 were variable and 1005 were conserved. The ML tree with the highest log likelihood (−8351.892) is shown in Fig. 5. The Bayesian likelihood score was −8330.051. The topology recovered by Bayesian analysis was identical to that of the ML tree.

Results from phylogenetic analyses indicated that our two strains (JCM 32617 and JCM 32616) were phylogenetically distinct from the other species belonging to the *D. arecae* complex. Their morphological features were also distinct from those of other species of the *D. arecae* complex [25]. Therefore, we establish the two new species as below.

3.2. Morphological analyses, taxonomy

Case 1 (Fig. 3)

Diaporthe oculi Mochiz. & Kaz. Tanaka, sp. nov.

MycoBank: MB 825540.

Sexual morph: Unknown. Asexual morph: Conidiomata pycnidial, scattered to 2–3 grouped, immersed, erumpent at the ostiolar neck, globose to depressed globose, 90–250 μm high, 110–310 μm diam, with yellow to pink conidial mass. Ostiolar neck

Fig. 3. *Diaporthe oculi* (HHUF 30565) in Case 1. a–f. Conidiomata, f. Conidioma with yellow sporulation, g, h. Longitudinal sections of conidiomata, i. Ostiolar neck, j–l. Conidiomatal walls at the base of ostiolar neck (j), side (k) and base (l), m–o. Conidiogenous cells, p, q. Alpha conidia. Scale bars: a–c = 2 mm, d–f = 500 μm, g = 50 μm, h = 100 μm, i–m = 20 μm, n–q = 5 μm.

cylindrical, central, 150–480 μm long, 80–140 μm diam, composed of rectangular, thick-walled, 2.5–12.5 × 2.5–7.5 μm, dark brown cells. Conidiomatal wall 5–8 μm thick at side, composed of 3–4 layers of 2.5–10 × 2–3 μm, flattened, pale brown cells; wall at the base of ostiolar neck 30–38 μm thick, composed of polygonal to rectangular, 2.5–12.5 × 2.5–5 μm, brown cells. Paraphyses absent. Conidiophores reduced to conidiogenous cells. Conidiogenous cells are cylindrical to lageniform, 6–15 × 2–5 μm, phialidic. Alpha

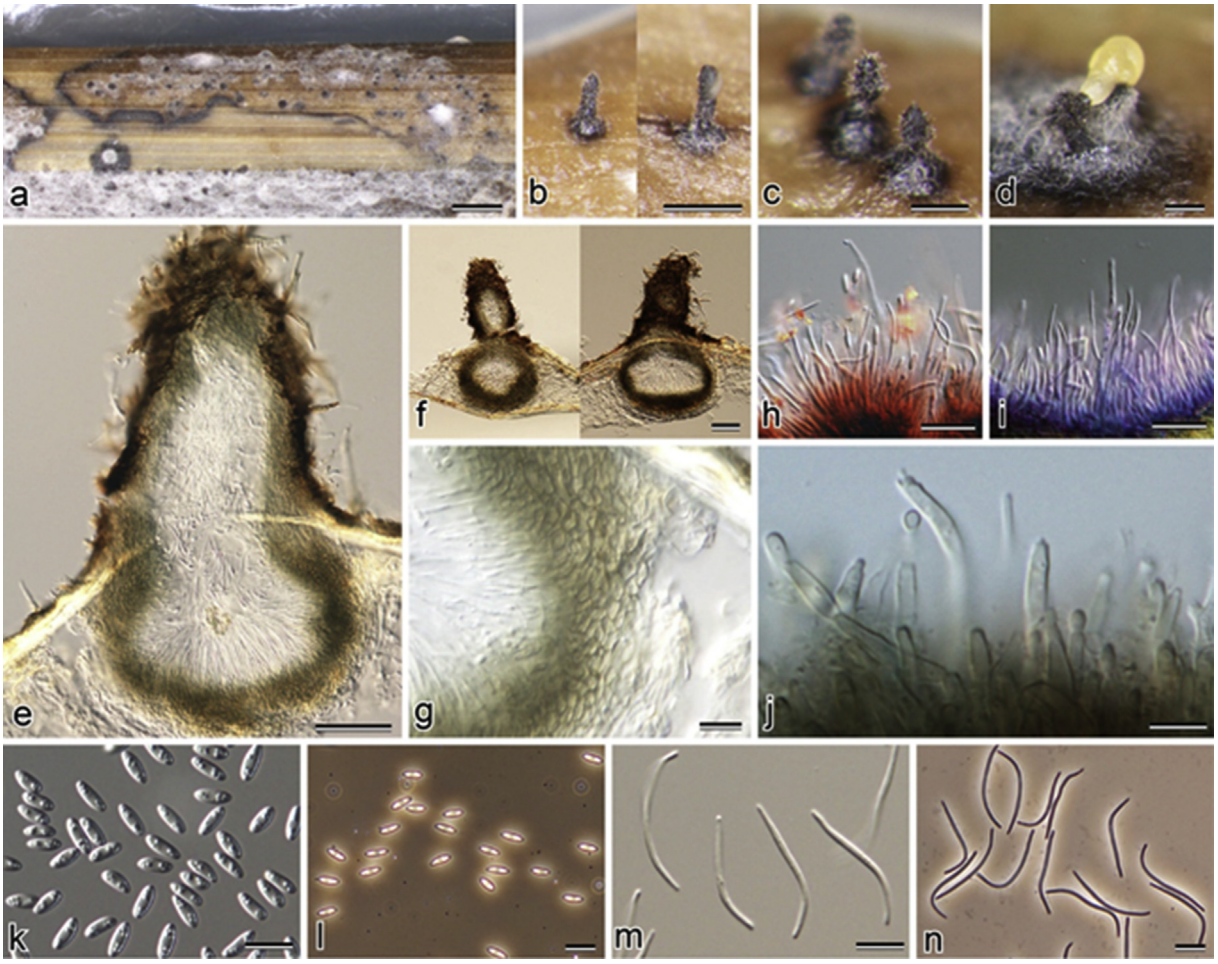

Fig. 4. *Diaporthe pseudooculi* (HHUF 30617) in Case 2. a–d. Conidiomata (d. Conidioma with yellow sporulation), e, f. Longitudinal sections of conidiomata, g. Conidiomatal wall, h–j. Conidiophores and conidiogenous cells, k, l. Alpha conidia, m, n. Beta conidia. Scale bars: a = 1 mm, b = 500 μm, c, d = 200 μm, e, f = 50 μm, g, k–n = 10 μm, h, i = 20 μm, j = 5 μm.

conidia fusoid-ellipsoid, 5–8.5 × 2–3 μm (av. 6.7 × 2.4 μm, n = 50), l/w 2.3–3.2 (av. 2.7 n = 50), hyaline, aseptate. Beta and gamma conidia not observed.

***Specimen examined*:** Japan, Gifu, Gifu University, mycelial isolate from diseased human eye, culture Gifu_U_D = JCM 32617 = MAFF 246252 (Dried culture specimen, HHUF 30565 holotype designated here).

Sequences: LC373514 (ITS), LC373516 (*tef1*), and LC373518 (*TUB*).

Case 2 (Fig. 4)

Diaporthe pseudooculi Mochiz. & Kaz. Tanaka, sp. nov.

MycoBank: MB 825541.

Sexual morph: Unknown. Asexual morph: Conidiomata pycnidial, scattered to 2–3 grouped, immersed, erumpent at the ostiolar neck, globose to depressed globose, 220–330 μm high, 180–280 μm diameter with white to yellow conidial mass. Ostiolar neck cylindrical to papillate, central, 100–220 μm long, 45–130 μm diameter. Conidiomatal wall 12–20 μm thick at side, composed of 2.5–10 × 2–5 μm, flattened, polygonal cells. Paraphyses filamentous, 50–65 μm long, 1.5–2.5 μm wide. Conidiophores hyaline, 5–12 × 2–5 μm. Conidiogenous cells cylindrical, 12–18 × 2 μm, phialidic. Alpha conidia ellipsoid, 6–9 × 2–3.5 μm (av. 7.3 × 2.8 μm, n = 50), l/w 2.1–3.2 (av. 2.6, n = 50), hyaline, aseptate. Beta conidia sigmoid, 21.5–33.5 × 1.2–1.7 μm (av. 27.0 × 1.4 μm, n = 30), aseptate, hyaline. Gamma conidia not observed.

***Specimen examined*:** Japan, Gifu, Gifu University, mycelial isolate from diseased human eye, culture Gifu_U_68M = JCM 32616 = MAFF 246452 (Dried culture specimen, HHUF 30617 holotype designated here).

Sequences: LC373515 (ITS), LC373517 (*tef1*), and LC373519 (*TUB*).

3.3. Fungal identification

A BLAST analysis of the 3-gene sequence alignment showed that each isolated fungus differed from known species, and the morphological features of the isolates were not consistent with any *Diaporthe*. We identified our isolates as new *Diaporthe* species based on molecular and morphological data.

3.4. In vitro antifungal susceptibility testing

The MICs to AMPH-B, flucytosine, FLCZ, ITCZ, miconazole, MCFG, VRCZ, and pimaricin for Case 1 were; 0.25, >64, 64, 1.0, 2.0, 0.03, <0.015, and 2.0 μg/mL respectively. For Case 2, they were 0.25, >64, >64, 1.0, 2.0, 0.06, 0.12, and 4.0 μg/mL respectively. These are reference values because there was no established method of testing the susceptibility of the *Diaporthe* species.

4. Discussion

Although *Diaporthe* is very prevalent in nature, they rarely cause human disease. Earlier reports said that infections of *Diaporthe* species were caused in patients who were treated with

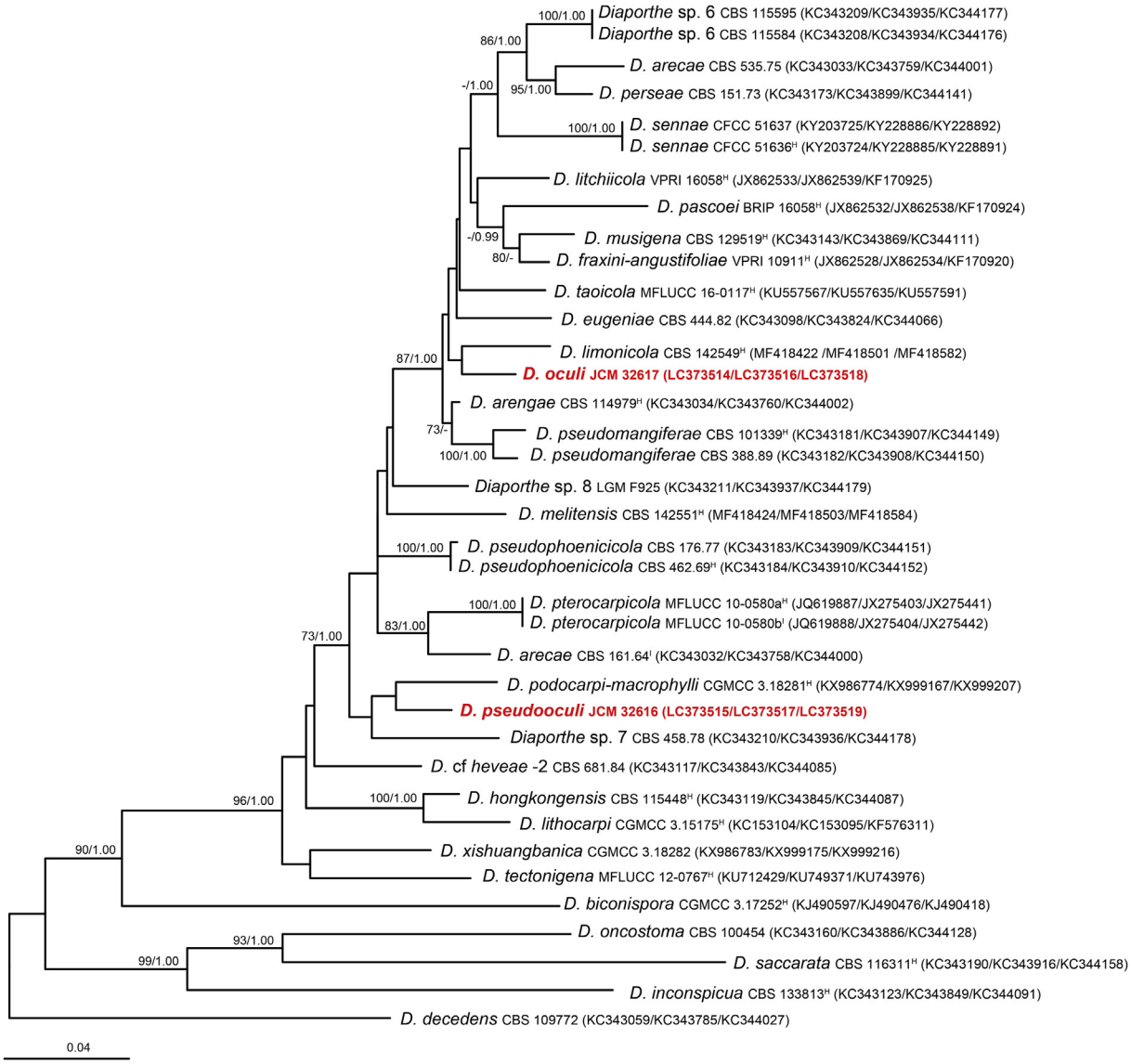

Fig. 5. Maximum-likelihood (ML) tree of *Diaporthe arecae* complex based on the ITS-*tef1*-*TUB* sequences. An ML bootstrap proportion (BP) greater than 70% and Bayesian posterior probabilities (PP) above 0.95 are presented at the nodes as ML BS/Bayesian PP. A hyphen ("-") indicates values lower than 70% BP or 0.95 PP. Ex-holotype and isotype strains are indicated with superscripts H and I respectively. The newly obtained sequences are shown in bold and red. Numbers following the taxon names represent GenBank accession. The scale bar represents nucleotide substitutions per site.

immunosuppression drugs [4–8]. It suggested that the pathogenicity of *Diaporthe* species was not strong.

Only two cases of ocular infections with *Diaporthe* species were reported previously (Table 1) [9,10]; a case of mycotic scleral keratitis caused by *Diaporthe phoenicicola* 6 weeks after pterygium surgery [10,26] and a case of fungal keratitis caused by unidentified *Diaporthe* that resulted from a rose thorn injury [9]. In our Case 2, the rose thorn injury led to fungal infection, similar to a previous report [9]. Although the patient did not have an obvious injury in Case 1, his hobby was gardening and he had a history of pterygium surgery. The relationships between fungal scleral keratitis and pterygium surgery also have been reported [10,27–30]. Hsiao CH et al. reported that the latency period between the time of pterygium excision and the onset of infectious scleritis was 8.9 ± 10.5 years (range, 1 week to 32 years) [27]. Singh RP et al. reported a sclerokeratitis case 10 years after pterygium excision with mitomycin C [30]. The use of cytotoxic drug such as mitomycin C during pterygium surgery destroys conjunctival and episcleral tissue, and also blood vessels. In case 1, we did not know whether adjunctive therapy such as mitomycin C was used during the pterygium operation or not. However, we suspected that these eyes might be susceptible to infection by bacteria or fungi because of the pterygium surgery causing an absence of protective tissue and blood supply [27]. And it is well known that topical steroids exacerbate keratomycosis [31,32]. Although the Case 1 patients did not have a traumatic episode, he had diabetes mellitus and was prescribed topical steroids as an initial therapy. We suspected these factors enabled to anchor *Diaporthe* species on ocular surface and to be keratomycosis.

In Case 1, the causal fungus was identified as a new species of *Diaporthe*, and was named *D. oculi*. It can be distinguished from the closely related *D. limonicola* on *Citrus limon* (Rutaceae) by the ITS, *tef1*, and *TUB* (515/520 = 99.0% in ITS, 315/324 = 97.2% in *tef1*, and 601/614 = 97.9% in *TUB*). Paraphyses and beta and gamma conidia reported for *D. limonicola* [33] were not observed in *D. oculi*. Morphologically, *D. oculi* is similar to *D. arengae* found from *Arenga*

Table 1
Summary of the publications of human invasive infection caused by *Diaporthe* sp.

Reference	Gender/Age[a]	Species	Clinical presentation	DM[b]	Therapy		Others[d]	Relation with plant
					Surgery	Antifungal agents[c]		
Sutton (1999)	F/61	*Diaporthe* sp.	osteomyelitis	+	incised and drained	FLCZ, ITCZ	rheumatoid arthritis treated with steroid and methotrexate	gardener
Mandell (2009)	M/63	*Diaporthe* sp.	keratitis	–	keratoplasty	VRCZ, AMPH-B	topical steroid	rose thorn injury, gardener
Iriart (2011)	M/60	*D. phaseolorum*	osteomyelitis	–	–	ITCZ	HTLV-1	farmer
Gajjar (2011)	M/48	*D. phoenicicola*	keratitis	–	–	natamycin, FLCZ	pterygium surgery	–
Garcia-Reyne (2011)	F/72	*D. longicolla*	cutaneous infection	–	amputation	ITCZ, terbinafine, VRCZ	renal transplant	–
Cariello (2013)	M/61	*D. bougainvilleicola*	bursitis	+	debridement	VRCZ	renal transplant, HCV hepatitis treated with IFN	farmer
Mattei (2013)	M/43	*D. phaseolorum*	cutaneous infection	+	surgically excised	ITCZ	renal transplant	farmer
Rakita (2017)	M/79	*D. eres/D. nobilis*	cutaneous infection	–	surgically excised	posaconazole,	heart transplant	gardener
This study	M/81	*D. oculi*	keratitis	+	keratoplasity	VRCZ,L-AMB	pterygium surgery	gardener
	M/68	*D. pseuooculi*	keratitis	+	–	VRCZ,L-AMB	–	rose thorn injury, gardener

[a] "M": male, "F": female.
[b] "DM": diabetes mellitus.
[c] "FLCZ": fluconazole, "AMPH–B": amphotericin B, "VRCZ": voriconazole, "ITC": itraconazole Z, "L–AMB": liposomal amphotericin B.
[d] "HTLV–1": Human T-cell leukemia virus type 1, "HCV": hepatitis C virus, "IFN": interferon.

engleri (Arecaceae), but the latter species has longer conidiophores up to 60 μm and beta conidia [34]. The isolate from Case 2 was also identified as a new *Diaporthe* species, *D. pseudooculi*. Phylogenetically, *D. pseudooculi* is different from the closely related *D. podocarpi-macrophylli* by the ITS, *tef1*, and *TUB* (525/531 = 98.9% in ITS, 314/333 = 94.3% in *tef1*, and 436/442 = 98.6% in *TUB*). It differs from *D. podocarpi-macrophylli* isolated from healthy leaves of *Podocarpus macrophyllus* (Podocarpaceae) in the longer beta conidia (vs. 8.5–31.5 μm; [35]).

These two new *Diaporhte* species share close phylogenetic affinities with *D. arecae* species complex [25] but were scattered in different clades in the analysis of the combined dataset (Fig. 5). Although measurements of the alpha conidia are similar in these two new species, the absence of paraphyses and beta conidia differentiate *D. oculi* from *D. pseudooculi*. These species have the same habit, the human eye, and the pathogenicity of these species is another point interest. Due to the limited number of infectious cases, however, the detail of their virulence is not yet to be known. Further study is warranted.

In the earlier cases with *Diaporhte* species, diverse therapies have been used because the optimal treatment had not been established (Table 1) [3–10]. The antifungal susceptibility of keratomycosis seemed to be different from those of subcutaneous infections. The scleral keratitis caused by *D. phoenicicola* responded well to topical natamycin (pimaricin) and oral FLCZ [10]. The case of *Diaporthe* sp. keratitis was successfully treated by a combination of penetrating keratoplasty and topical VRCZ and AMPH-B therapy [9]. Although Case 1 eventually needed keratoplasty, topical and systemic VRCZ were effective. Case 2 was treated with topical VRCZ, AMPH-B, and pimaricin with intravenous VRCZ. Both isolates had good susceptibility to AMPH-B, VRCZ, ITCZ, and MCFG similar to previous results [9]. We tested the isolates by broth microdilution following the modified CLSI M38-A2 standard. Further studies are needed to standardize antifungal susceptibility testing of filamentous fungi especially species of *Diaporthe*.

In conclusions, two new species of *Diaporthe* capable of causing human diseases particularly keratomycosis were found.

Conflicts of interest

All authors declare that he/she has no conflict of interest.

Ethical approval

All procedures performed in these studies involving human participants were in accordance with the ethical standards of the Institutional and/or National Research Committee and with the 1964 Declaration of Helsinki and its later amendments or comparable ethical standards.

This article does not contain any studies with animals performed by any of the authors.

Informed consent

Informed consent was obtained from all individual participants included in the study.

References

[1] Nielsen SE, Nielsen E, Julian HO, Lindegaard J, Højgaard K, Ivarsen A, et al. Incidence and clinical characteristics of fungal keratitis in a Danish population from 2000 to 2013. Acta Ophthalmol 2015;93:54–8.
[2] Homa M, Shobana CS, Singh YR, Manikandan P, Selvam KP, Kredics L, et al. Fusarium keratitis in South India: causative agents, their antifungal susceptibilities and a rapid identification method for the *Fusarium solani* species complex. Mycoses 2013;56:501–11.

[3] Iriart X, Binois R, Fior A, Blanchet D, Berry A, Cassaing S, et al. Eumycetoma caused by *Diaporthe phaseolorum* (*Phomopsis phaseoli*): a case report and a mini-review of *Diaporthe/Phomopsis* spp invasive infections in humans. Clin Microbiol Infect 2011;17:1492–4.
[4] Sutton DA, Timm WD, Morgan-Jones G, Rinaldi MG. Human phaeohyphomycotic osteomyelitis caused by the coelomycete *Phomopsis Saccardo* 1905: criteria for identification, case history, and therapy. J Clin Microbiol 1999;37:807–11.
[5] Mattei AS, Severo CB, Guazzelli LS, Oliveira FM, Gené J, Guarro J, et al. Cutaneous infection by *Diaporthe phaseolorum* in Brazil. Med Mycol Case Rep 2013;8:85–7.
[6] Rakita RM, O'Brien KD, Bourassa L. *Diaporthe* soft tissue infection in a heart transplant patient. Transpl Infect Dis 2017;19. https://doi.org/10.1111/tid.12680. https://doi.org/10.1111/tid.12680.
[7] Garcia-Reyne A, López-Medrano F, Morales JM, García Esteban C, Martín I, Eraña I, et al. Cutaneous infection by *Phomopsis longicolla* in a renal transplant recipient from Guinea: first report of human infection by this fungus. Transpl Infect Dis 2011;13:204–7.
[8] Cariello PF, Wickes BL, Sutton DA, Castlebury LA, Levitz SM, Finberg RW, et al. *Phomopsis bougainvilleicola* prepatellar bursitis in a renal transplant recipient. J Clin Microbiol 2013;51:692–5.
[9] Mandell KJ, Colby KA. Penetrating keratoplasty for invasive fungal keratitis resulting from a thorn injury involving Phomopsis species. Cornea 2009;28:1167–9.
[10] Gajjar DU, Pal AK, Parmar TJ, Arora AI, Ganatra DA, Kayastha FB, et al. Fungal scleral keratitis caused by *Phomopsis phoenicicola*. J Clin Microbiol 2011;49:2365–8.
[11] Tanaka K, Hirayama K, Yonezawa H, Hatakeyama S, Harada Y, Sano T, et al. Molecular taxonomy of bambusicolous fungi: tetraplosphaeriaceae, a new pleosporalean family with Tetraploa-like anamorphs. Stud Mycol 2009;64:175–209.
[12] White TJ, Bruns T, Lee S, Taylor J. Amplification and direct sequencing of fungal ribosomal RNA genes for phylogenetics. In: Innis MA, Gelfand DH, Sninsky JJ, White TJ, editors. PCR Protocols: a guide to methods and applications. San Diego, U.S.A: Academic Press; 1990. p. 315–22.
[13] Carbone I, Kohn LM. A method for designing primer Sets for speciation studies in filamentous ascomycetes. Mycologia 1999;91:553–6.
[14] Glass NL, Donaldson GC. Development of primer sets designed for use with the PCR to amplify conserved genes from filamentous ascomycetes. Appl Environ Microbiol 1995;61:1323–30.
[15] O'Donnell K, Cigelnik E. Two divergent intragenomic rDNA ITS2 types within a monophyletic lineage of the fungus Fusarium are nonorthologous. Mol Phylogenet Evol 1997;7:103–16.
[16] Katoh K, Rozewicki J, Yamada KD. MAFFT online service: multiple sequence alignment, interactive sequence choice and visualization. Briefings Bioinf 2017:bbx108. https://doi.org/10.1093/bib/bbx108.
[17] Tanabe AS. Kakusan4 and Aminosan: two programs for comparing nonpartitioned, proportional and separate models for combined molecular phylogenetic analyses of multilocus sequence data. Mol Ecol Resour 2011;11:914–21.
[18] Akaike H. A new look at the statistical model identification. IEEE Trans Automat Contr 1974;19:716–23.
[19] Schwarz G. Estimating the dimension of a model. Ann Stat 1978;6:461–4.
[20] Miller MA, Schwartz T, Pickett BE, He S, Klem EB, Scheuermann RH, et al. A RESTful API for access to phylogenetic tools via the CIPRES science Gateway. Evol Bioinform 2015;11:43–8.
[21] Stamatakis A. RAxML version 8: a tool for phylogenetic analysis and post-analysis of large phylogenies. Bioinform 2014;30:1312–3.
[22] Ronquist F, Teslenko M, van der Mark P, Ayres DL, Darling A, Höhna S, et al. MrBayes 3.2: efficient bayesian phylogenetic inference and model choice across a large model space. Syst Bio 2012;61:539–42.
[23] Rambaut A, Suchard MA, Xie W, Drummond AJ. Tracer v. 1.6. 2014. Accessed 2016; May 27, http://tree.bio.ed.ac.uk/software/tracer/.
[24] Gao Y, Liu F, Cai L. Unravelling Diaporthe species associated with camellia. Syst Biodivers 2016;14:102–17.
[25] Huang F, Udayanga D, Wang X, Hou X, Mei X, Fu Y, et al. Endophytic Diaporthe associated with Citrus: a phylogenetic reassessment with seven new species from China. Fungal Biol 2015;119:331–47.
[26] Dhanushka U, Xingzhong L, Crous Pedro W, Eric H, McKenzie C, Chukeatirote Ekachai, et al. A multi-locus phylogenetic evaluation of Diaporthe (Phomopsis). Fungal Divers 2012;56:157–71.
[27] Hsiao CH, Chen JJ, Huang SC, Ma HK, Chen PY, Tsai RJ. Intrascleral dissemination of infectious scleritis following pterygium excision. Br J Ophthalmol 1998;82:29–34.
[28] Kumar B, Crawford GJ, Morlet GC. *Scedosporium prolificans* corneoscleritis: a successful outcome. Aust N Z J Ophthalmol 1997;25:169–71.
[29] Peponis V, Rosenberg P, Chalkiadakis SE, Insler M, Amariotakis A. Fungal scleral keratitis and endophthalmitis following pterygium excision. Eur J Ophthalmol 2009;19:478–80.
[30] Singh RP, McCluskey P. *Scedosporium* prolificans sclerokeratitis 10 years after pterygium excision with adjunctive mitomycin C. Clin Exp Ophthalmol 2005;33:433–4.
[31] Mitsui Y, Hanabusa J. Corneal infections after cortisone therapy. Br J Ophthalmol 1955;39:244–50.
[32] Isobe Y. The effect of topical steroid medication on experimental candida keratitis. Nippon Ganka Gakkai Zasshi 1991;95:45–51.
[33] Guarnaccia V, Crous PW. Emerging citrus diseases in Europe caused by species of Diaporthe. IMA Fungus 2017;8:317–34.
[34] Gomes RR, Glienke C, Videira SI, Lombard L, Groenewald JZ, Crous PW. Diaporthe: a genus of endophytic, saprobic and plant pathogenic fungi. Persoonia 2013;31:1–41.
[35] Gao Y, Liu F, Duan W, Crous PW, Cai L. Diaporthe is paraphyletic. IMA Fungus 2017;8:153–87.